Proceedings of the 11th World Congress on Electrical Engineering and Computer Systems and Sciences (EECSS'25)
Paris, France - August, 2025
Paper No. CIST 104
DOI: 10.11159/CIST25.104

Development of AI Control Technology for Laser Keyhole Welding

Ikuo TANABE[1], Hiromi ISOBE[2]
[1]Sanjo City University
5002-5 Kamisugoro, Sanjo, Niigata, Japan
tanabe.ikuo@sanjo-u.ac.jp
[2] Nagaoka University of Technology
1603-1 Kamitomioka, Nagaoka, Niigata, Japan
Isobe163@mech.nagaokaut.ac.jp

Abstract **-** Laser welding is widely used in a variety of fields, including the automotive, aerospace, and electronics industries. In laser keyhole welding, large energy is irradiated over a small area, making it extremely difficult to find the optimum processing conditions to achieve the desired welding specifications. In particular, the search for optimum processing conditions is difficult in the overlap welding of thin plates, and a great deal of time and effort is required to find the best conditions. Overlap welding of thin plates can be done reliably with FSW (Friction Stir Welding), however it requires long processing time and a wide welding allowance, thus increasing the product size. Therefore, in this research, new AI control technology for laser keyhole welding was developed and evaluated. A neural network was used for AI control technology. The neural network using the data of laser keyhole welding with thin SUS 304 plats was firstly developed. And its neural network has been rewritten as an algebraic formula. A program with C language was then created to use that algebraic formulation to search for the optimum conditions on laser processing. As a result, it had been concluded that the proposed new AI control technology for laser keyhole welding could calculate with high accuracy for the desired welding processing conditions, and the proposed technology is very effective for the search of the optimum processing conditions.

Keywords**:** AI control, Laser keyhole welding, Overlap welding of thin plates, Optimum processing conditions,

1. Introduction

Laser processing is widely used in various fields such as automotive, aerospace, and electronics industries [1-3]. Laser welding irradiates a large amount of energy onto a small area, making it extremely difficult to find the optimal processing conditions to achieve the desired welding specifications [4-6]. In particular, it is difficult to find the optimum processing conditions for lap welding of thin plates, and the search for the optimum processing conditions requires a great deal of time and labour. On the other hand, there has been a recent demand for technology for lap welding of thin aluminium and stainless-steel plates for battery housings of electric vehicles [7]. FSW (=Friction Stir Welding) can be used to reliably weld these thin plates together, but the long processing time makes it extremely difficult to be productive. In addition, the product size is large due to the large area of the joining area [8].

In this study, a new AI (= Artificial Intelligence) control technique for laser keyhole welding was developed and evaluated. First, a neural network model was constructed using data from the overlap welding of two stainless-steel sheets as teacher data. Next, the neural network model was rewritten into an algebraic formulation, and a program was written in C language to search for optimal processing conditions for laser welding of overlapping thin plates using the algebraic formulation. Finally, the effectiveness of the proposed method was evaluated by experiments.

2. Description of Laser Keyhole Welding

Laser welding is a welding process in which a laser beam is irradiated to a workpiece locally for a short time. It is necessary to supply a sufficient amount of energy for melting, but control on the millisecond order is required to prevent insufficient melting or, conversely, fusion breakdown. A keyhole is a cavity generated by evaporation on the workpiece surface directly under the torch, which enables deep penetration welding. This welding process is also prone to spatter (dispersal of molten metal during welding). The stainless-steel SUS304 used in this research is also a keyhole weld.

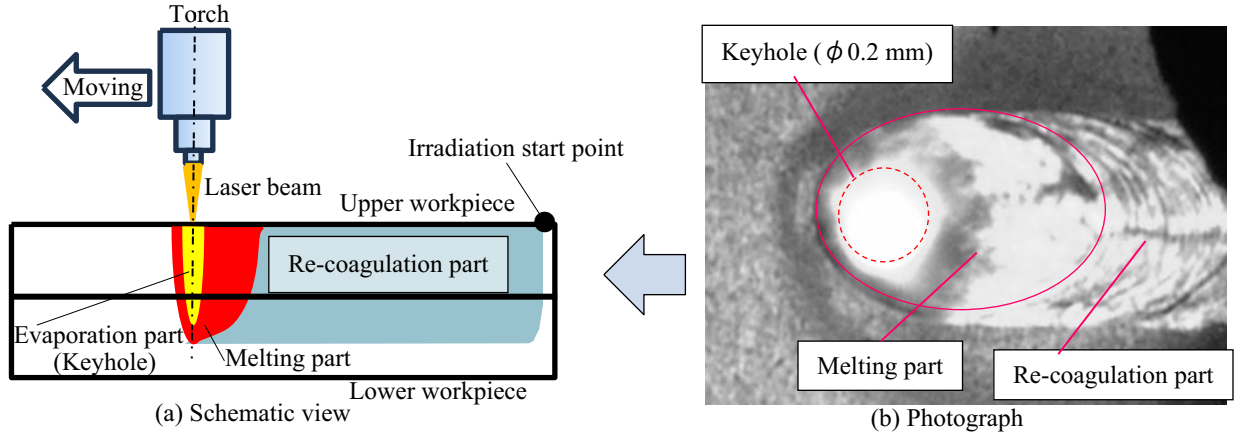

Fig. 1: Schematic view and photograph of the keyhole type welding.

Figure 1(a) shows a schematic view of keyhole welding by laser traveling irradiation, and Figure 1(b) shows a photograph of keyhole welding. keyholes generated by the evaporation of SUS304 move as the laser travels. There is a molten area of SUS304 around the keyhole, and the molten area also moves along with the movement of the keyhole. This molten area is wider on the opposite side of the travel direction due to the laser travel irradiation, and is used to bury the keyhole after the torch travels.

3. AI Control Technology for Searching Optimal Processing Conditions in Laser Keyhole Welding

An AI control system for searching optimal processing conditions in laser keyhole welding has been developed using neural networks as the AI control technology. A neural network model was constructed using data from the overlap welding of two stainless-steel (SUS304) sheets with a thickness of 3 mm as teacher data, the model was rewritten into an algebraic formulation, and a program was created in C language to search for optimal processing conditions using the algebraic formulation.

3.1. Development of Neural Network Model for AI Control

A neural network model for AI control has been developed. Figure 2 shows the developed neural network model. It is a neural network with three structures: an input layer with 5 points, an hidden layer with 45 points, and an output layer with

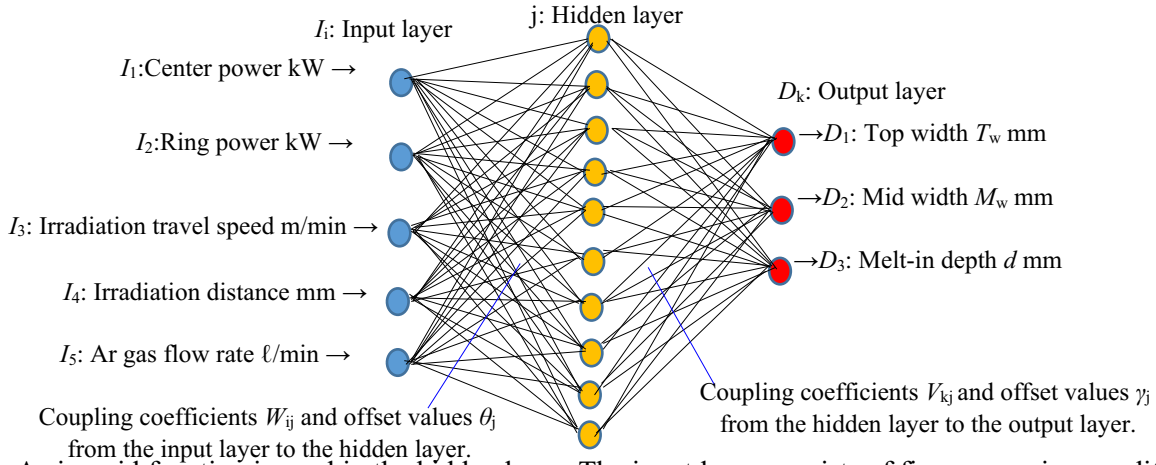

Fig. 2: Neural network model for AI control of laser keyhole welding.

3 points. A sigmoid function is used in the hidden layer. The input layer consists of five processing conditions I_i (I_1: centre power kW, I_2: ring power kW, I_3: irradiation travel speed m/min, I_4: irradiation distance mm, I_5: Ar gas flow rate ℓ/min). The

output layers were set to three melt-in specifications, D_k (D_1: top width T_w mm, D_2: mid width M_w mm, D_3: melt-in depth d mm) (See Fig. 5).

Overlap laser welding of two 3 mm × 150 mm × 100 mm stainless-steel plates (SUS304, melting point 1450°C, boiling point 2862°C) as shown in Figure 3 was performed using the Ring-type laser torch shown in Figure 4 and the processing conditions in Table 1, to obtain the teacher data. Argon gas was used as the assist gas to prevent oxidation. As the final characteristic values of the teacher data, as shown in Figure 5, three welding specifications required for welding stainless-steel plates in overlap welding were measured: the welding top width T_w, the welding depth d, and the welding width M_W of the joining surface. Table 2 shows an example of 65 pieces of teacher data, showing the relationship between laser welding process conditions and welding specifications. Since this teacher data includes the factor of "uncertainty" of laser welding described in Chapter 2, it is considered that the neural network constructed using this teacher data can calculate the causal relationship between processing conditions and welding specifications, taking the "uncertainty" into account.

Neural network training uses the steepest descent method to obtain the minimum sum of squares of the difference between teacher data and output data by modifying the coupling functions W_{ji} and V_{kj} between units and the offset values θ_j

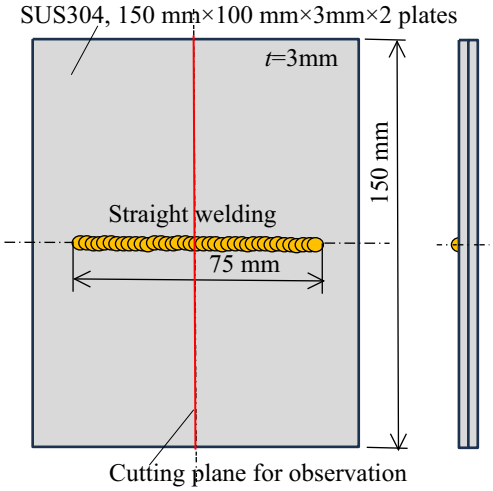

Fig. 3: Schematic view of the experiment for the teacher data.

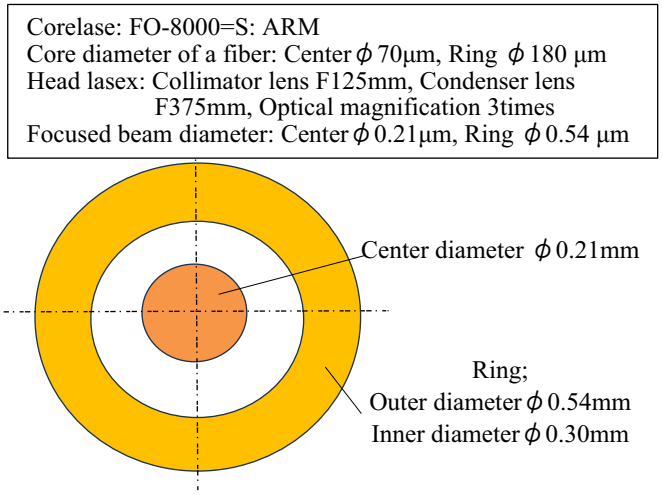

Fig. 4: Specification of the ring type laser torch.

Table: 1 Laser keyhole welding conditions for neural network teacher data.

Laser processing machine	Fiber laser processing
Center power	0.3 ～ 1.5 (kW)
Ring power	0.0 ～ 2.6 (kW)
Irradiation travel speed	0.5, 1.0, 2.0 (m/min)
Ar gas flow rate	20, 30 (ℓ/min)
Irradiation distance	366, 367, 368,369, 370(mm)

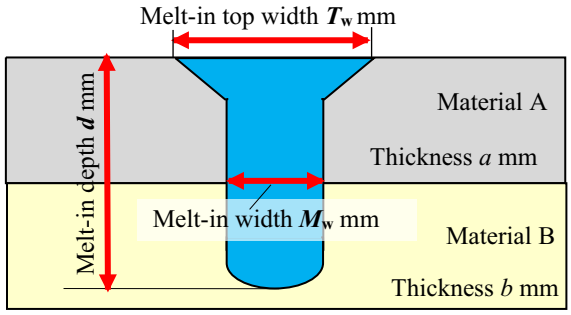

Fig. 5: Definition of quality evaluation factors for laser key-hole welding.

Table 2: Processing conditions and an experimental result of laser key hole welding of SUS304 (melting specifications).

Laser processing conditions					Experimental results (melting specifications)		
Center Power kW	Ring Power kW	Irradiation travel speed m/min	Ar gas flow rate ℓ/min	Irradiation distance mm	Top width T_w mm	Mid width M_w mm	Melt-in depth d mm
1.1	2.1	1.0	30	366	3.6	1.1	4.6

and γ_k between units sequentially in the program. W_{ji} is the coupling function between the input and intermediate layers, V_{kj} is the coupling function between the intermediate and output layers, θ_j is the offset value to the intermediate layer, and γ_k is the offset value to the output layer. The back-propagation method was used here. The error function E_p of the training pattern p is shown in Equation (1).

$$E_p = \frac{1}{2}\sum_k (T_{kp} - D_{kp})^2 \tag{1}$$

Where T_{kp} is the teacher data of unit k for training pattern p and D_{kp} is the output data of unit k for training pattern p. The training patterns are the melting-in specifications after laser welding (D_1: top width T_w mm, D_2: mid width M_w mm, D_3: melt-in depth d mm). The neural network model in Figure 2 was trained using 65 pairs of teacher data sets. As a result, the value of the error function E_p was reduced to 1.7×10^{-29} after 10000 learning cycles, which is considered to be convergence. In order to promote convergence, both centre power and ring power, which are considered to have a direct influence, were adjusted by a factor of 1000 times, physically taking into account the causal relationship between the processing conditions and welding specifications. Ar gas flow rate and irradiation distance, which are considered to have an indirect effect, were both adjusted by a factor of 0.001 times.

3.2. Algebraic Formulation of the Constructed Neural Network

The algebraic formulation is obtained using the neural network model in the previous section. The coupling functions W_{ji} and offset values θ_j from the input layer to the intermediate layer of the constructed neural network, and the coupling functions V_{kj} and offset values γ_k from the intermediate layer to the output layer of the constructed neural network were う used for that, respectively. Relationship between the coupling functions W_{ji}, V_{kj}, the offset values θ_j, γ_k and the welding-in specification D_k (D_1: top width T_w mm, D_2: mid width M_w mm, D_3: melt-in depth d mm) is shown in Equation (2).

$$D_k = \sum_{j=1}^{\text{Hidden layer num.}} \frac{V_{kj}}{1 + \exp\left\{-\sum_{i=1}^{\text{Input layer num.}} (W_{ij} I_i) + \theta_j\right\}} + \gamma_k \tag{2}$$

Where I_1 is centre power kW, I_2 is ring power kW, I_3 is Irradiation travel speed m/min, I_4 is Irradiation distance mm, and I_5 is Ar gas flow rate ℓ/min. By inputting the five processing conditions I_i into Equation (2), the welding-in specification D_k can be easily calculated. However, the centre power 1000 times, ring power 1000 times, Ar gas flow rate 0.001 times, and Irradiation distance 0.001 times are also required here.

3.3. Creation of a Programme to Search for Optimum Processing Conditions for Laser Keyhole Welding of Overlapping Thin Plates

Using the neural network algebraically formulated in the previous section, a program was created to quickly and easily search for optimal processing conditions for laser keyhole welding of overlapping thin plates. The program was written in the C language. Figure 6 shows a flowchart of the program.

First, the available range of processing conditions I_i (centre power I_1 kW, ring power I_2 kW, irradiation travel speed I_3 m/min, irradiation distance I_4 mm, Ar gas flow rate I_5 ℓ/min) and the number of calculation steps for each processing condition in (i), then the desired welding specifications and their allowable ranges (top width $T_w \pm \Delta T_w$ mm, mid width $M_w \pm \Delta M_w$ mm and melt-in depth $d \pm \Delta d$ mm) are entered in (ii).

Next, the neural network formulation (2) is used to calculate the welding specification D_k (D_1: top width T_w mm, D_2: mid width M_w mm and D_3: melt-in depth d mm) and this calculated value is used to search for the desired welding specification D_k in (ii). Only when the calculated values are within the allowable range of the welding specifications entered

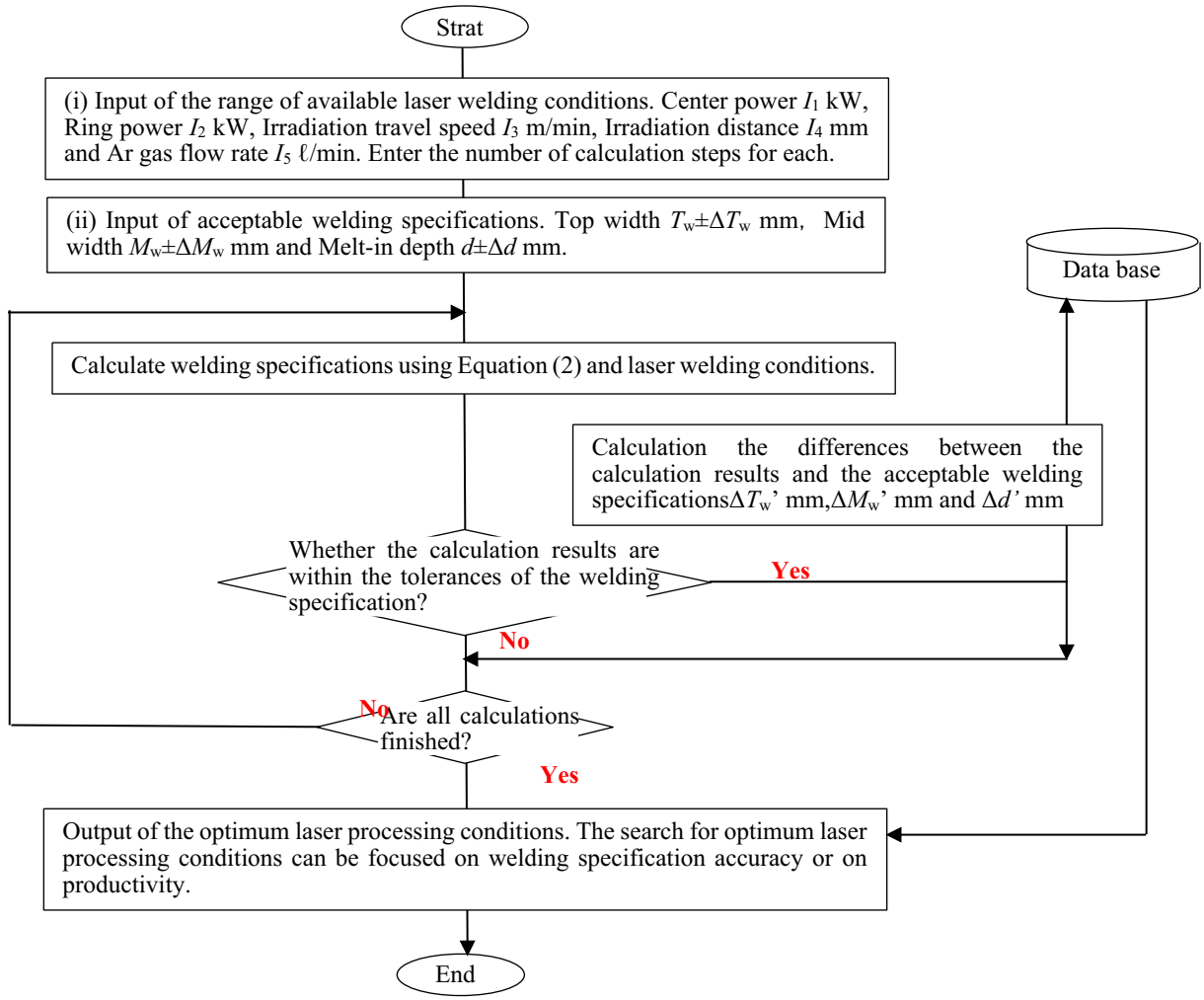

Fig.6: Flow chart of program for searching of the optimum laser processing conditions regarding the overlapping keyhole welding of thin sheets.

in (ii), the difference from the desired welding specifications (ΔT_w' mm, ΔM_w' mm, and Δd ' mm) is calculated and registered in the database. This is done for all combinations of conditions within the input machining condition area. Finally,

the database is accessed and the optimum machining conditions are output (on screen or printed if desired). The search for optimum processing conditions includes two types of conditions: one that emphasizes welding specification accuracy (conditions in which $|\Delta T_w'$ mm$| + |\Delta M_w'$ mm$| + |\Delta d'$ mm$|$ is as small as possible) and one that emphasizes productivity (conditions in which Irradiation (Irradiation travel speed I_3 m/min as large as possible). In both cases, the optimal processing conditions are displayed in pooled-down order from the best processing condition in the search for welding specification accuracy, and in descending order from the best processing condition in the search for productivity. The welding-in specification D_k (D_1: top width T_w mm, D_2: mid width M_w mm, D_3: melt-in depth d mm) for each machining condition is also shown.

This made it possible to search very quickly and easily for the optimum processing conditions for laser keyhole welding of overlapping thin plates. The total calculation time, including input and calculation time, was about a few minutes, even for a complete beginner. (The PC used had the following performance: OS is Windows XP, CPU is Intel(R) Core2 Duo 2.4GHz, memory is 2GB).

4. Evaluation Experiments for the Proposed Technology

This chapter describes the evaluation of a program that searches for optimum processing conditions for laser welding of overlapping thin plates. First, two types of input data shown in Table 3 were input to the program created in Section 3.3, and the optimum processing conditions were searched for as shown in Table 4 that specified "emphasis on welding specification accuracy. The total calculation time was about 2 minutes (The PC used had the following performance: OS is Windows XP, CPU is Intel(R) Core2 Duo 2.4GHz, memory is 2GB)), and the optimal processing conditions were quickly found.

Table 3: Input data for laser welding conditions and acceptable welding specifications for evaluation.

Test No.	Range of available laser welding conditions and calculation steps for each					Acceptable welding specifications		
	Centre Power kW	Ring Power kW	Irradiation travel speed m/min	Ar gas flow rate ℓ/min	Irradiation distance mm	Top width T_w mm	Mid width M_w mm	Melt-in depth d mm
1	0.5 ~ 1.0, Step 0.1	0.5 ~ 2.0 Step 0.1	0.5 ~ 1.0 Step 0.1	30	366 ~ 377 Step 1.0	3.6±0.1	1.1±0.1	4.6±0.1
2	0.5 ~ 1.0, Step 0.1	0.5 ~ 2.0 Step 0.1	0.5 ~ 1.0 Step 0.1	30	366 ~ 377 Step 1.0	4.4±0.1	1.5±0.1	4.5±0.1

Table 4: Calculated results for the optimum laser welding conditions and calculation times.

Test No.	Calculated laser welding conditions					Calculation times		
	Centre Power kW	Ring Power kW	Irradiation travel speed m/min	Ar gas flow rate ℓ/min	Irradiation distance mm	Time for data input min	Calculation time min	Total time min
I	1.0	2.0	1.0	30	366	2.0	3.1	5.1
II	0.5	1.7	0.5	30	370	2.0	3.2	5.1

(a) Surface

(b) Back

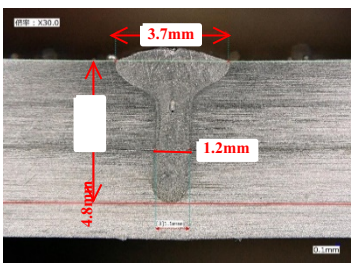

(c) Cross-section

(a) Surface (b) Back (c) Cross-section

Fig. 8: Photograph after laser welding__Test No. II.

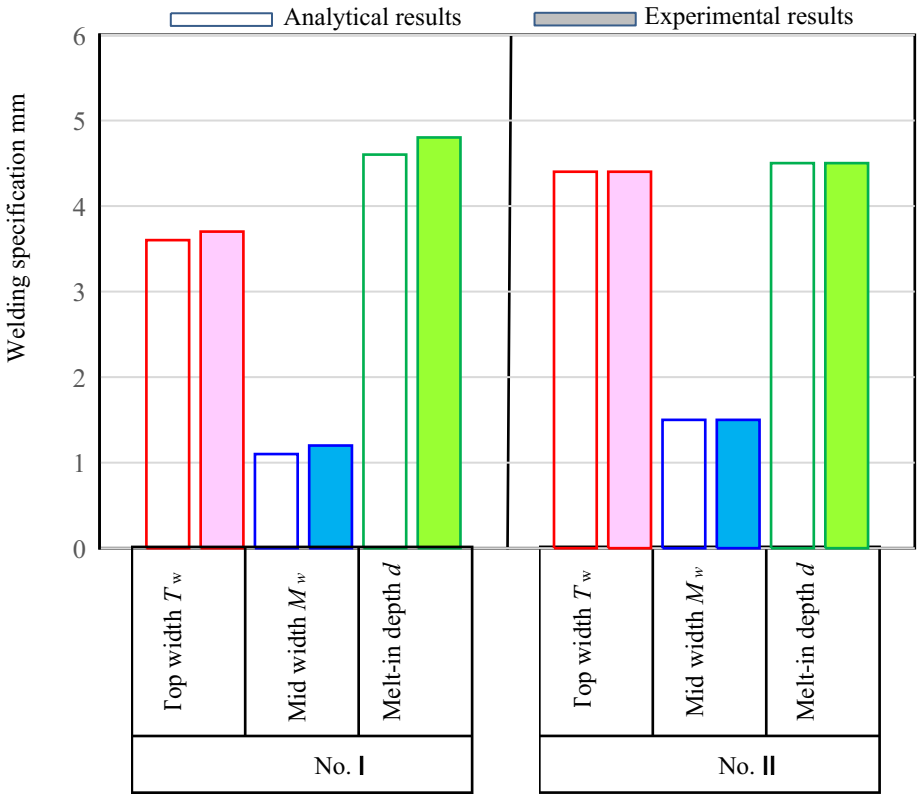

Fig. 9: Comparison of calculated and experimental results for evaluation of the developed

Figure 7 and Figure 8 show the experimental results of the explored laser processing conditions, respectively. Figure 9 shows the calculated and experimental results of the weld-in specification. It is clear that the calculated and experimental results correspond relatively well. The desired values, the calculation results, and the experimental results correspond well,

indicating that the optimal machining condition search program was able to search for machining conditions that emphasize welding specification accuracy. Thus, the proposed technology can be effectively used industrially.

As described above, AI control technology has been developed for overlap laser keyhole welding of SUS 304 with two plates thickness of 3 mm, and it has been shown that welding specifications can be controlled with high precision. In the next report, the AI control technology will be reported with the addition of aluminium as the material and 1 mm and 2 mm as the plate thickness to increase versatility.

5. Conclusion

A new AI control technique for laser keyhole welding was developed and evaluated. The results are summarized as follows; (1) The neural network used in the AI control technology was able to simulate the overlap welding of two thin stainless-steel plates with high accuracy. (2) The neural network with algebraic formulation was able to calculate the welding specifications (top width: T_w mm, mid width: M_w mm, melt-in depth: d mm) quickly, easily, and accurately. (3) The developed program was evaluated to be industrially effective because it was able to search for optimal welding conditions with a high degree of accuracy, focusing on the accuracy of welding specifications and on productivity.

References

[1] GUAN, G., "Evaluation of Selective Laser Sintering Processes by Optical Coherence Tomography," Materials and Design, vol. 88, pp. 837–846, 2015.

[2] KROLIKOWSKI M., PRZESTACKI D., CHWALCZUK T., SOBOLEWSKA E., TOMASIK M., "Additive Manufacturing of Polyether Ether Ketone – Peek Parts with Surface Roughness Modification by A Laser Beam," Journal of Machine Engineering, ISSN 1895-7595 (Print) ISSN 2391-8071 (Online), vol. 20, no.3, pp. 117–124, 2020.

[3] PEYRE P., "Experimental and Numerical Analysis of the Selective Laser Sintering (SLS) of PA12 and PEKK Semi-Crystalline Polymers," Journal of Materials Processing Technology, vol. 225, pp. 326–336, 2015.

[4] MILLER R., DEBROY T., "Energy absorption by metal-vapor dominated plasma during carbon dioxide laser welding of steels," Journal of Applied Physics, vol. 68, no.5, pp. 2045-2050, 1990.

[5] SETO N., KATAYAMA S., MATSUNAWA A., "High-speed simultaneous observation of plasma and keyhole behaviour during high power CO_2 laser welding: Effect of shielding gas on porosity," Journal of Laser Applications, vol. 12, no. 6, pp. 245-250, 2000.

[6] MARTIN R. M., OKMOTO Y., OKADA A., MATTI N., JARNO K., JORMA V., "High surface quality welding of aluminium using adjustable ring-mode fibre laser," Journal of Materials Processing Technology, vol. 258, pp. 180-188, 2018.

[7] NHK, Web feature, Electric vehicles, https://www3.nhk.or.jp/news/html/20221116/k10013893081000.html, (Reference date August 23, 2024.).

[8] TWI, COREFLOWTM, A SUB-SURFACE MACHINING PROCESS, https://www.twi-global.com/media-and-events/insights/coreflow-a-sub-surface-machining-process, (Reference date August 23, 2024.).